

Surface characterization of sulfate, molybdate, and tungstate promoted TiO₂-ZrO₂ solid acid catalysts by XPS and other techniques

Benjaram M. Reddy^{a,*}, Pavani M. Sreekanth^a, Yusuke Yamada^b,
Qiang Xu^b, Tetsuhiko Kobayashi^{b,1}

^a *Inorganic and Physical Chemistry Division, Indian Institute of Chemical Technology, Hyderabad 500 007, India*

^b *National Institute of Advanced Industrial Science and Technology (AIST), 1-8-31 Midorigaoka, Ikeda, Osaka 563-8577, Japan*

Received 1 October 2001; received in revised form 26 November 2001; accepted 27 November 2001

Abstract

Titania–zirconia binary oxide supported sulfate, molybdate, and tungstate promoted solid acid catalysts were prepared by suspending the hydrous mixed oxide support in aqueous solutions of sulfuric acid, ammonium heptamolybdate, and ammonium metatungstate. The suspensions were refluxed at 383 K followed by evaporation of the water, drying and calcination at 1073 K. The resulting materials were characterized by means of X-ray powder diffraction, BET surface area, FT-Raman, and X-ray photoelectron spectroscopy methods. The calcined TiO₂-ZrO₂ binary oxide, X-ray amorphous at 773 K, forms a definite crystalline ZrTiO₄ compound at 1073 K. The XRD measurements further reveal the presence of Ti₂(SO₄)₃ and Zr(SO₄)₂ compounds in the case of SO₄²⁻/TiO₂-ZrO₂ sample and Zr(MoO₄)₂ and Zr(WO₄)₂, respectively, in the case of molybdenum- and tungsten-oxide promoted catalysts. The FT-Raman results also support these observations. The XPS measurements show peak broadening and shift in the binding energies of O 1s, Ti 2p, and Zr 3d lines in the case of sulfated catalyst. The characterization results indicate that the impregnated sulfate ion shows a relatively strong influence on the physicochemical properties of the TiO₂-ZrO₂ mixed oxide, which is followed by molybdate. © 2002 Elsevier Science B.V. All rights reserved.

Keywords: Solid superacid; Titania–zirconia; Mixed oxide; Sulfate ion; Molybdenum oxide; Tungsten oxide; X-ray diffraction; FT-Raman; X-ray photoelectron spectroscopy

1. Introduction

The sulfate ion doped zirconia (SO₄²⁻/ZrO₂) as a solid superacid has attracted much attention recently because of its interesting catalytic applications [1,2]. The sulfated zirconia was reported to be very active in

the isomerization of *n*-butane and aliphatic alkylation reactions even at room temperature. These catalysts were also utilized for other reactions, such as polymerization of ethers [3], acetylation of toluene and benzene with acyl chloride [4], benzylation of toluene with benzyl chloride [5], esterification of alcohol with acetic acid [6], and benzylation of toluene with benzyl chloride [7]. It is an established fact in the literature that the catalytic activity of superacids for many reactions of hydrocarbon transformations is surprisingly high [8,9]. They can even activate methane at low

* Corresponding author. Fax: +91-40-717-3387.

E-mail addresses: bmreddy@iict.ap.nic.in (B.M. Reddy), t-kobayashi@aist.go.jp (T. Kobayashi).

¹ Co-corresponding author. Fax: +81-727-51-9630.

temperature. As catalyst, solid superacids have some additional advantages, such as ease of separation from a reaction mixture, no corrosion of the reaction equipment, and free from environmental pollution, etc. Hino and Arata [10], and Arata and Hino [11] further reported that the solid superacids could be synthesized by supporting WO_3 or MoO_3 on ZrO_2 or TiO_2 under certain preparation conditions. Our recent investigations also revealed that the molybdate or tungstate doped ZrO_2 catalysts exhibit very interesting catalytic activity for various organic synthesis and transformation reactions in the liquid phase [12–14]. These solid acids can remain stable even at high temperature and in a solid–liquid system. Therefore, these catalysts have better application prospects than many other solid superacids such as SbF_5 or sulfate supported on metal oxides.

The isomerization of linear alkanes has received great attention as a way to improve the octane number of gasoline, due to the limited amounts of benzene currently accepted. Sulfated zirconia, with or without platinum, has been studied as an alternative catalyst to the commercial Pt/mordenite [15,16]. Sulfur leaching during reaction would probably prevent the commercial use of sulfate-promoted zirconia. A new tungsten-oxide promoted zirconia ($\text{WO}_x\text{-ZrO}_2$) was considered as an alternative catalyst for the skeletal isomerization of alkanes and its high activity was related to the superacidity of this catalyst system [10].

The use of binary oxides such as $\text{TiO}_2\text{-ZrO}_2$ in the place of ZrO_2 may be very interesting. They exhibit relatively high BET surface area, high thermal stability, and high mechanical strength [17,18]. The $\text{TiO}_2\text{-ZrO}_2$ binary oxide has also been reported to exhibit a high surface acidity by a charge imbalance based on the generation of Ti–O–Zr bonding [19,20]. Further, recent studies reveal that $\text{TiO}_2\text{-ZrO}_2$ is an active catalyst for dehydrocyclization of *n*-paraffins, isomerization of alkanes, hydrogenation of carboxylic acids to alcohols, and also effective support for MoO_3 -based catalysts for hydroprocessing applications [17,21,22]. Thus, the combined $\text{TiO}_2\text{-ZrO}_2$ mixed oxide has attracted much attention recently as a catalyst and support for various applications. As in the case of ZrO_2 , the addition of various dopants such as sulfate, molybdate, and tungstate could be expected to show very strong influence on the surface acid–base properties of these materials [19,23]. Therefore, a

comprehensive investigation of the influence of various dopants on the physicochemical properties of $\text{TiO}_2\text{-ZrO}_2$ mixed oxides is highly essential in view of their commercial implications. The present investigation was undertaken to fill this gap. The primary objective of this study was to understand the precise role of sulfate, molybdate, and tungstate on the physicochemical characteristics of the $\text{TiO}_2\text{-ZrO}_2$ binary oxide. For this purpose, a hydrated titania–zirconia was prepared by a coprecipitation method and doped with sulfate, molybdate, and tungstate promoters and investigated by X-ray diffraction, FT-Raman, and X-ray photoelectron spectroscopy techniques. The preliminary results of this investigation are reported in this short communication.

2. Experimental

2.1. Catalyst preparation

The $\text{TiO}_2\text{-ZrO}_2$ binary oxide (1:1 mol ratio based on oxides) was prepared by a homogeneous coprecipitation method with in situ generated ammonium hydroxide by decomposition of urea at 368 K. For this purpose, an aqueous solution containing the requisite quantities of TiCl_4 (Fluka, AR grade), ZrOCl_2 (Fluka, AR grade), and urea (Loba Chemie, GR grade) were heated together to 368 K with vigorous stirring. In about 6 h of heating, as decomposition of urea progressed to a certain extent, the pH of the solution increased from 2 to more than 7 and the formation of precipitate gradually occurred. The precipitate was heated for 6 h more to facilitate aging. The resulting precipitate was filtered off, washed several times with deionized water until free from chloride ions, and dried at 393 K for 12 h. A portion of the oven-dried material was calcined at 1073 K for 5 h in air atmosphere and stored in dry nitrogen atmosphere.

To incorporate the sulfate ion the oven dried hydrous titania–zirconia (6 g) was immersed in 0.5 M H_2SO_4 solution (30 ml) for 30 min. The excess water was evaporated on a water bath and the resulting sample was oven dried at 393 K for 12 h and calcined at 1073 K for 5 h and stored in dry nitrogen atmosphere. The molybdate and tungstate promoted $\text{TiO}_2\text{-ZrO}_2$ catalysts, containing 10 wt.% MoO_3 or WO_3 were prepared by a suspension impregnation method. To

incorporate molybdenum- or tungsten-oxide, the required quantities of ammonium heptamolybdate (Fluka, AR grade) or ammonium metatungstate (J.T. Baker, UK, GR grade) were dissolved in excess water and the finely powdered oven dried hydrous titania–zirconia support was added to this solution and refluxed at 383 K for 2 h. The excess water was then evaporated on a water-bath with continuous stirring. The resulting sample was oven dried at 393 K for 12 h and calcined at 1073 K for 5 h in air atmosphere and stored in dry nitrogen atmosphere.

2.2. Catalyst characterization

X-ray powder diffraction patterns have been recorded on a Siemens D-5000 instrument by using Cu K α radiation source and scintillation counter detector. The XRD phases present in the samples were identified with the help of JCPDS data files. The specific surface area of the samples was determined on a conventional standard static volumetric high vacuum (1×10^{-4} Pa) system by N₂ physisorption at liquid N₂ temperature and by taking 0.162 nm² as the molecular area of N₂ molecule. Before measurements, the samples were dried in situ at 473 K for 2 h under vacuum. Raman spectra were recorded at ambient temperature on a Nicolet FT-Raman 960 spectrometer with a range of 4000–100 cm⁻¹ and a spectral resolution of 2 cm⁻¹ using the 1064 nm exciting line (~600 mV) of a Nd:YAG laser (Spectra Physics, USA). Finely powdered samples were contained in a 5 mm o.d. NMR tube. Before measurements, samples were dried in a vacuum oven for several hours. The XPS measurements were made on a Shimadzu (ESCA 3400) spectrometer by using Mg K α (1253.6 eV) radiation as the excitation source. The spectra were recorded after argon-ion etching for 1 min (2 kV, 30 mA). Charging of catalyst samples was corrected by setting the binding energy of adventitious carbon (C 1s) at 284.6 eV [24,25]. The finely ground oven dried samples were dusted on a double stick graphite sheet and mounted on the standard sample holder. The sample holder was then transferred to the analysis chamber, which can house ten samples at a time, through a rod attached to it. The XPS analysis was done at room temperature and pressures typically in the order of less than 10⁻⁶ Pa. The samples were out gassed in a vacuum oven overnight before XPS measurements.

3. Results and discussion

The X-ray powder diffraction patterns of undoped TiO₂-ZrO₂ binary oxide and various promoted TiO₂-ZrO₂ samples are shown in Fig. 1. The formation of crystalline ZrTiO₄ compound can be clearly noted (JCPDS file no. 7-290) in the case of unpromoted TiO₂-ZrO₂ mixed oxide sample. Our earlier investigation [18] on various TiO₂-ZrO₂ samples calcined at different temperatures revealed that the TiO₂-ZrO₂ mixed oxide is in an amorphous or poorly crystalline state up to the calcination temperature of 873 K. However, the formation of crystalline ZrTiO₄ compound starts beyond 873 K. Further, the intensity of the lines due to ZrTiO₄ compound increased with increasing calcination temperature up to 1273 K. The ZrTiO₄ was found to be thermally quite stable up to 1273 K in the absence of any additive atoms [26]. Recently, Fung and Wang [17] also reported the formation of ZrTiO₄ compound at 923 K and above temperatures. Noguchi and Mizuno [27] have reported that tetragonal and monoclinic ZrO₂ and rutile TiO₂ could be formed by the decomposition of ZrTiO₄ compound at higher temperatures. Wu et al. [28] also reported the formation of TiO₂ (rutile) phase at higher calcination temperatures. No independent lines due to TiO₂ (anatase or rutile) and ZrO₂ (monoclinic, tetragonal, or cubic) phases were observed in the present study in agreement with our earlier studies [18,26]. As envisaged earlier, the observed higher stability of ZrTiO₄ compound is mainly due to a different preparation method adopted and the precursor compounds used for the preparation of the binary oxide support. In the case of sulfate ion impregnated TiO₂-ZrO₂ sample, in addition of the lines of ZrTiO₄ compound a few extra lines due to the formation of Ti₂(SO₄)₃ (JCPDS file no. 22-947) and Zr(SO₄)₂ (JCPDS file no. 20-1474) compounds can be noted. In the case of molybdenum- and tungsten-oxide promoted catalysts, the formation of Zr(MoO₄)₂ (JCPDS file no. 21-1496) and Zr(WO₄)₂ (JCPDS file no. 31-1500) compounds, in addition to the ZrTiO₄ compound, can be noted. To confirm the presence of various compounds, these samples were further calcined at 1273 K for 5 h and subjected to XRD analysis. A further improvement in the intensity of the lines assigned to these phases was noted [26]. Thus, the XRD measurements reveal that the investigated promoter atoms show a strong

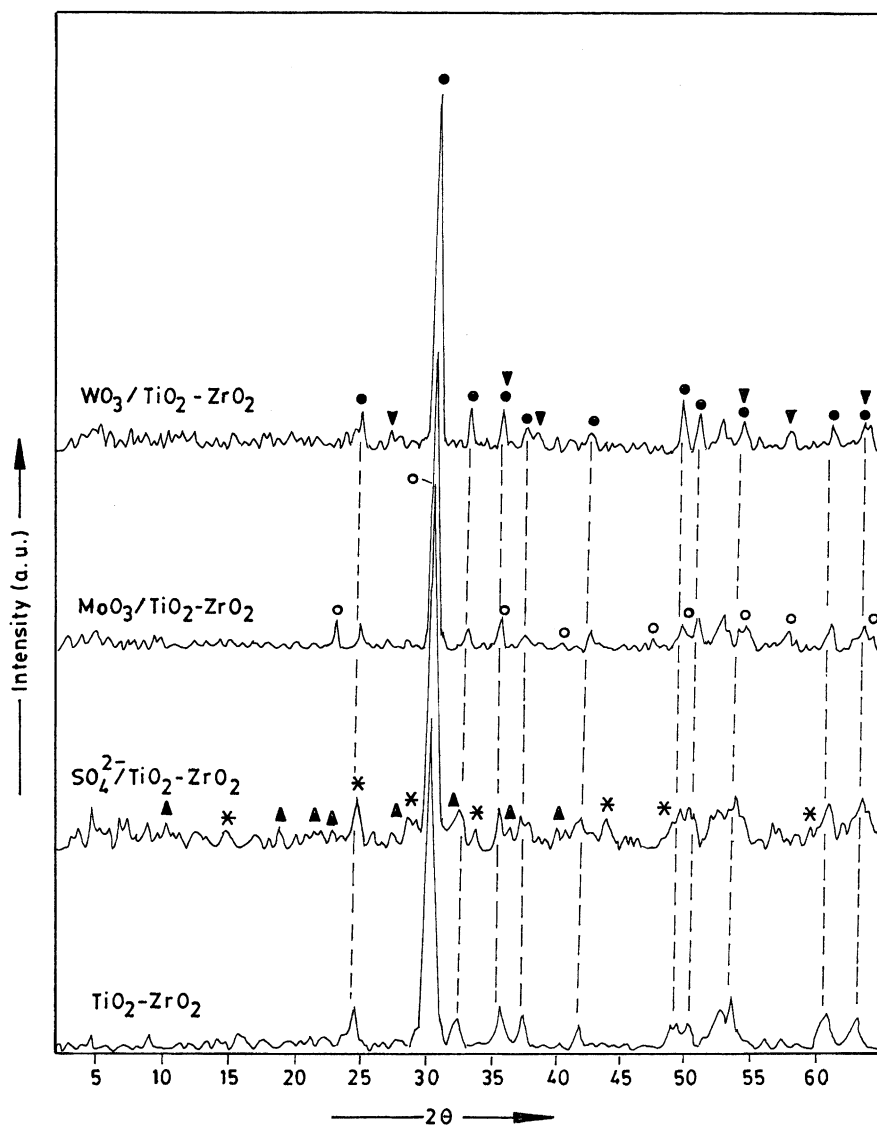


Fig. 1. X-ray powder diffraction patterns of $\text{TiO}_2\text{-ZrO}_2$ and promoted $\text{TiO}_2\text{-ZrO}_2$ samples calcined at 1073 K: characteristic lines due to (●) ZrTiO_4 ; (*) $\text{Ti}_2(\text{SO}_4)_3$; (▲) $\text{Zr}(\text{SO}_4)_2$; (○) $\text{Zr}(\text{MoO}_4)_2$; (▼) $\text{Zr}(\text{WO}_4)_2$.

but similar influence on the bulk properties of the titania–zirconia binary oxide support.

The FT-Raman spectra of various samples are presented in Fig. 2. The spectrum of undoped $\text{TiO}_2\text{-ZrO}_2$ contains broad bands at around 135, 168, 280, 338, 412, 640 and 803 cm^{-1} which should be characteristic for a ZrTiO_4 compound. To establish the evaluation of ZrTiO_4 compound, the $\text{TiO}_2\text{-ZrO}_2$ mixed

oxide was calcined at 773, 873, 973 and 1073 K for 6 h, respectively, and the Raman spectra were recorded. This study clearly established the fact that the titania–zirconia mixed oxide transforms from an amorphous to a crystalline compound beyond 873 K with reasonably well resolved Raman bands. Fung and Wang [17] also reported that the $\text{TiO}_2\text{-ZrO}_2$ was amorphous when it was calcined at temperatures less

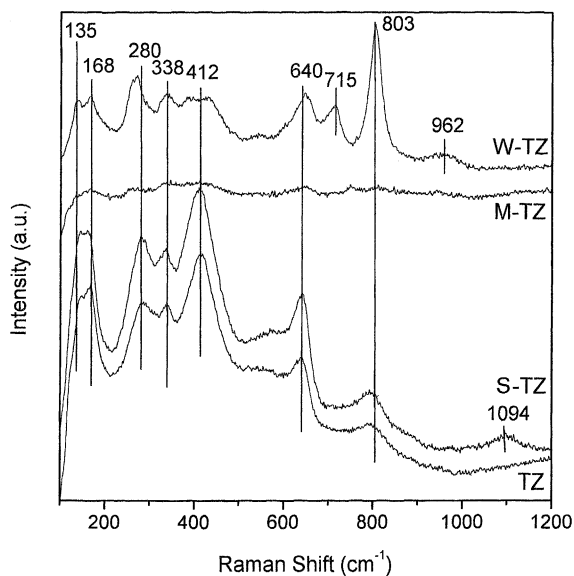


Fig. 2. FT-Raman spectra of $\text{TiO}_2\text{-ZrO}_2$ and promoted $\text{TiO}_2\text{-ZrO}_2$ samples calcined at 1073 K: (TZ) $\text{TiO}_2\text{-ZrO}_2$; (S-TZ) $\text{SO}_4^{2-}/\text{TiO}_2\text{-ZrO}_2$; (M-TZ) $\text{MoO}_3/\text{TiO}_2\text{-ZrO}_2$; (W-TZ) $\text{WO}_3/\text{TiO}_2\text{-ZrO}_2$.

than 873 K. The Raman spectrum of TiO_2 anatase exhibits bands at 144, 199, 399, 520, 638 and the TiO_2 rutile at 144 and 611 cm^{-1} , respectively [29]. Zirconia is known to exist in monoclinic, tetragonal and cubic modifications, and as an amorphous solid. The Raman spectra of monoclinic and tetragonal ZrO_2 exhibits bands at 103, 181, 190, 222, 310, 337, 382, 474, 499, 540, 559, 620, 636, 763 cm^{-1} and the shoulder at 261–270, respectively [30–32]. No characteristic bands for these individual component oxides can be noted. Thus, the FT-Raman results support the observations made from XRD study. In the case of promoted $\text{TiO}_2\text{-ZrO}_2$ sample, in addition to all the ZrTiO_4 Raman bands a few extra bands could be noticed due to the formation of various

compounds as observed from XRD study. The two-dimensional polymolybdate on various supports including ZrO_2 and TiO_2 gives a broad and characteristic Raman band at 960 cm^{-1} [33]. The crystalline MoO_3 on these supports shows sharp peaks at 820 and 995 cm^{-1} [32–35]. The absence of lines due to crystalline MoO_3 clearly indicate that the doped molybdate has strongly interacted with the support oxide. The spectrum of molybdenum-oxide promoted $\text{TiO}_2\text{-ZrO}_2$ is relatively very broad compared to that of other two samples. This sample is slightly gray in colour while other samples are white and transparent. Similarly, the microcrystalline WO_3 on various supports exhibit strong Raman bands at 807, 715 and 274 cm^{-1} [29]. No such defined bands can be noted in the case of tungsten-oxide promoted sample. However, a wide variety of octahedrally and tetrahedrally coordinated WO_x compounds show Raman bands in the range of $700\text{--}1060\text{ cm}^{-1}$ [36,37]. The presence of such bands gives an impression that those may be present on the surface of the binary oxide support. However, in broad terms the influence of various promoters on the surface of $\text{TiO}_2\text{-ZrO}_2$ mixed oxide is almost same. This may probably be the reason why all these materials exhibit similar solid acidity.

The N_2 BET surface areas of various samples are shown in Table 1. As can be noted from this table, there is a slight decrease in the BET surface area of the $\text{TiO}_2\text{-ZrO}_2$ sample after impregnating with sulfate ion. However, in the case of Mo- and W-oxide promoted samples, the loss in the BET surface area is substantial when compared to that of unpromoted $\text{TiO}_2\text{-ZrO}_2$. This may primarily be due to the formation of non-porous $\text{Zr}(\text{MoO}_4)_2$ and $\text{Zr}(\text{WO}_4)_2$ compounds at higher calcination temperature. A slightly high surface area could be one of the reasons for the observed high activity of sulfated catalyst when compared to that of other samples for various reactions [12,13].

Table 1

BET surface area ($\text{m}^2\text{ g}^{-1}$) and electron binding energies (eV) of $\text{TiO}_2\text{-ZrO}_2$ binary oxide support and various promoted $\text{TiO}_2\text{-ZrO}_2$ samples

Sample	BET surface area	O 1s	Ti 2p _{3/2}	Zr 3d _{5/2}	S 2p	Mo 3d _{5/2}	W 4f _{7/2}
$\text{TiO}_2\text{-ZrO}_2$	30	530.4	459.3	182.9	–	–	–
$\text{SO}_4^{2-}/\text{TiO}_2\text{-ZrO}_2$	28	531.3	459.7	183.2	167.4	–	–
$\text{MoO}_3/\text{TiO}_2\text{-ZrO}_2$	7	530.9	459.2	182.9	–	232.3	–
$\text{WO}_3/\text{TiO}_2\text{-ZrO}_2$	14	531.0	459.3	182.9	–	–	36.3

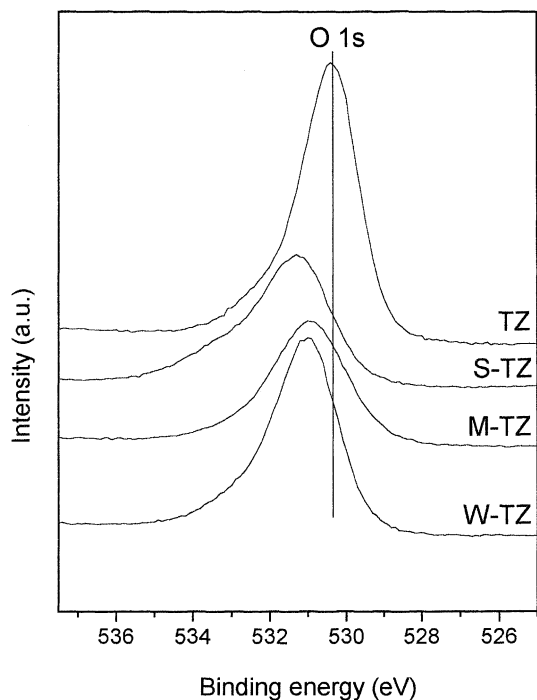


Fig. 3. The O 1s XPS spectra of $\text{TiO}_2\text{-ZrO}_2$ and promoted $\text{TiO}_2\text{-ZrO}_2$ samples calcined at 1073 K: (TZ) $\text{TiO}_2\text{-ZrO}_2$; (S-TZ) $\text{SO}_4^{2-}/\text{TiO}_2\text{-ZrO}_2$; (M-TZ) $\text{MoO}_3/\text{TiO}_2\text{-ZrO}_2$; (W-TZ) $\text{WO}_3/\text{TiO}_2\text{-ZrO}_2$.

The samples of unpromoted $\text{TiO}_2\text{-ZrO}_2$ and promoted $\text{TiO}_2\text{-ZrO}_2$ calcined at 1073 K have been investigated by XPS technique. The photoelectron peaks of O 1s, Ti 2p, and Zr 3d are shown in Figs. 3–5, respectively. The photoelectron spectra pertaining to S 2p, Mo 3d, and W 4f lines in various promoted catalysts have also been recorded, however, not shown in figures. The binding energies (E_b) of all the elements in these catalysts are shown in Table 1. As can be noted from Figs. 3–5 and Table 1 that the photoelectron peaks of these samples are sensitive to the nature of the promoter atoms. As shown in Fig. 3, the O 1s profile is, in general, more complicated due to the overlapping contribution of oxygen from titania and zirconia in the case of $\text{TiO}_2\text{-ZrO}_2$ sample and from sulfate, molybdate, and tungstate in addition to the oxides of titania and zirconia in the case of promoted catalysts. It can be noted from this figure that an extensive broadening of the O 1s peak of $\text{TiO}_2\text{-ZrO}_2$ sample after impregnating with promoter atoms. In particular, the extent of

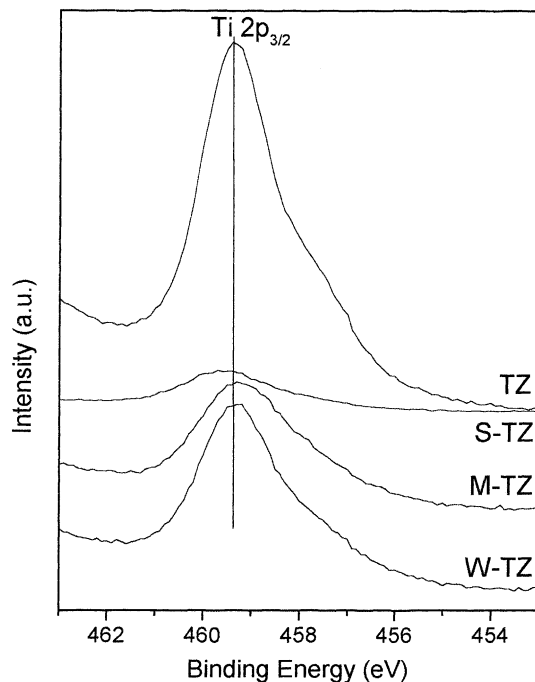


Fig. 4. The Ti 2p XPS spectra of $\text{TiO}_2\text{-ZrO}_2$ and promoted $\text{TiO}_2\text{-ZrO}_2$ samples calcined at 1073 K: (TZ) $\text{TiO}_2\text{-ZrO}_2$; (S-TZ) $\text{SO}_4^{2-}/\text{TiO}_2\text{-ZrO}_2$; (M-TZ) $\text{MoO}_3/\text{TiO}_2\text{-ZrO}_2$; (W-TZ) $\text{WO}_3/\text{TiO}_2\text{-ZrO}_2$.

peak broadening is more in the case of sulfated sample followed by Mo-oxide promoted sample. A similar decreasing trend in the O 1s peak intensity can also be noted in the case of the promoted catalysts. The XPS peak intensity depends on both ion density and its chemical environment. The oxygen ion density in various samples is expected to be same. Therefore, the decrease in the peak intensity can be attributed to different chemical environments. It is a known fact in the literature that the broadening of the ESCA peak depends on various factors including (i) the presence of more than one type of species with different chemical characteristics which cannot be discerned by ESCA; and (ii) electron transfer between the promoter and the support (metal oxide–support oxide interaction) [19,23,38]. The O 1s binding energies (Table 1) reveal that there is a slight increase in the binding energy of the $\text{SO}_4^{2-}/\text{TiO}_2\text{-ZrO}_2$ sample when compared to that of other samples due to the formation of respective metal sulfates.

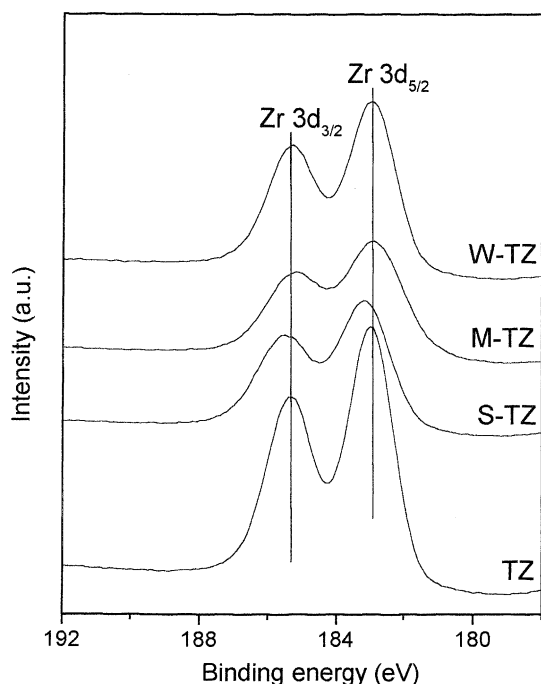


Fig. 5. The Zr 3d XPS spectra of $\text{TiO}_2\text{-ZrO}_2$ and promoted $\text{TiO}_2\text{-ZrO}_2$ samples calcined at 1073 K: (TZ) $\text{TiO}_2\text{-ZrO}_2$; (S-TZ) $\text{SO}_4^{2-}/\text{TiO}_2\text{-ZrO}_2$; (M-TZ) $\text{MoO}_3/\text{TiO}_2\text{-ZrO}_2$; (W-TZ) $\text{WO}_3/\text{TiO}_2\text{-ZrO}_2$.

Fig. 4 shows the binding energy of the Ti 2p photoelectron peak at around 459.3 eV for the Ti $2p_{3/2}$ line. Normally, the Ti $2p_{3/2}$ line in the case of unpromoted TiO_2 samples can be observed at 458.5 eV [19,23,39]. An increase in the binding energy of the same in the present study may be due to the formation of ZrTiO_4 compound. In particular, a slight shift to higher binding energy can be seen in the case of sulfated catalyst, which is mainly due to the formation of $\text{Ti}_2(\text{SO}_4)_3$ as observed from XRD study [25,40]. Very interestingly, the intensity of the Ti 2p core level spectra was also found to decrease substantially after impregnating with various promoters. Here again, the decrease in the intensity is more prominent in the case of sulfated catalyst than that of other samples. This observation once again gives an impression that the sulfate ion interacts very strongly with the $\text{TiO}_2\text{-ZrO}_2$ mixed oxide when compared to that of other promoters. It is quite obvious since the pH of the impregnating solutions are quite different. In the case of sulfate ion

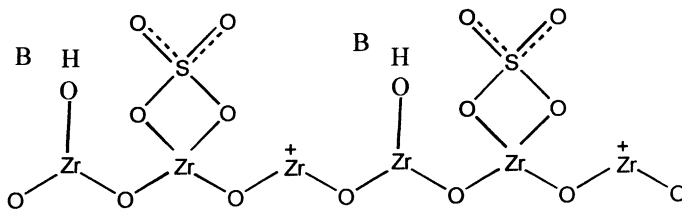
impregnated sample, the pH of the impregnating solution was about 2. However, in the case of molybdate and tungstate promoted samples, the ammonium salts of the corresponding metals exhibited the pH in the range of 7–8.

Fig. 5 shows the binding energy of the Zr 3d photoelectron peaks at 182.9 and 185.3 eV for Zr $3d_{5/2}$ and Zr $3d_{3/2}$ lines, respectively. The Zr 3d lines are well resolved with high intensity in the case of unpromoted $\text{TiO}_2\text{-ZrO}_2$ sample. However, a slight broadening and decrease in the intensity of the lines can be noted in the case of promoted catalysts. A slight shift towards higher binding energy can also be noted in the case of sulfate ion promoted sample. The binding energy of the Zr $3d_{5/2}$ line in undoped ZrO_2 sample ranges between 182.2 and 182.5 eV [25]. An increase in the binding energy of the Zr 3d line is mainly due to the formation of ZrTiO_4 compound in the case of unpromoted $\text{TiO}_2\text{-ZrO}_2$ sample, and the corresponding sulfate or metal oxide compounds in the case of promoted catalysts, respectively. Here too the sulfate ion has exhibited a strong influence on the intensity and binding energy of the Zr 3d lines in conformity with Ti 2p and O 1s spectra.

In the S 2p photoelectron spectrum of $\text{SO}_4^{2-}/\text{TiO}_2\text{-ZrO}_2$ sample two distinct 2p lines were observed corresponding to the sulfates of the individual metals reported in the literature [41]. However, the spectrum was more complicated due to the overlapping contribution between the Ti and Zr sulfates as observed in the case of O 1s line. The Mo $3d_{5/2}$ photoelectron peak of molybdenum-oxide promoted $\text{TiO}_2\text{-ZrO}_2$ sample was observed at 232.3 eV. Although, well-resolved Mo 3d lines were observed, however, they are very broad. The core level binding energy values indicate that the molybdenum is present in Mo(VI) state in the catalyst. As envisaged earlier the broadening of the ESCA peak can be attributed to various factors including (i) the presence of more than one type of Mo(VI) with different chemical characteristics; and (ii) electron transfer between active component and the support. As noted from XRD study, the molybdenum-oxide promoted $\text{TiO}_2\text{-ZrO}_2$ sample contains a well-defined $\text{Zr}(\text{MoO}_4)_2$ compound and the precursor of which, the amorphous Zr-O-Mo, may also be expected to present [35]. The broadening of the Mo 3d line clearly indicates the presence of both. As presented in Table 1, the W $4f_{7/2}$

photoelectron peak of tungsten-oxide promoted $\text{TiO}_2\text{-ZrO}_2$ catalyst was observed at 36.3 eV which agrees well with the values reported in the literature for tungsten compounds [25,42]. Here too, the W 4f spectrum was not well resolved indicating a lack of well-defined W(VI) species. As pointed out earlier, there could be several reasons for the observed extensive broadening of the XPS peaks. Which indicate clearly that in addition to the $\text{Zr}(\text{WO}_4)_2$ compound, there are some undefined WO_x species on the surface of the binary oxide support [37].

Various explanations can be found in the literature on the origin of solid acidity in the case of sulfate, molybdate, and tungstate doped zirconia catalysts [1,37,43]. In particular, the surface acidity characterization of $\text{SO}_4^{2-}/\text{ZrO}_2$ shows that its surface contains very strong Brønsted as well as Lewis acid sites. The number and the strength of these sites largely vary with parameters such as sulfur concentration, activation temperature and surface area of the precursor oxide. Based on IR and XPS techniques, Ward and Ko [44] have given the following structure of sulfated zirconia explaining the presence of both Brønsted and Lewis acid sites:



where B and Zr^+ are Brønsted and Lewis acid sites, respectively.

The Brønsted acid sites result from the weakening of the O–H bond by the neighboring sulfate groups, whereas the Lewis acid sites are electronically deficient Zr^{4+} centers as a result of the electron-withdrawing nature of the sulfate group. The situation will be very interesting in the case of $\text{TiO}_2\text{-ZrO}_2$ binary oxide where Zr–O–Ti linkages are expected to be present [19,23]. Therefore, the sulfate ion may coordinate to the surface of the $\text{TiO}_2\text{-ZrO}_2$ binary oxide having Zr–O–Ti linkages and form the support sulfate surface species like the one observed on the ZrO_2 support. In this case more surface acidity could be expected on the binary oxide support than that of ZrO_2 alone. However, to understand this

fact further studies are highly essential. Of course, the present characterization results provide evidence for the formation of $\text{Ti}_2(\text{SO}_4)_3$ and $\text{Zr}(\text{SO}_4)_2$ compounds also after impregnating with SO_4^{2-} ions on the surface of the binary oxide support.

Earlier research on molybdenum-oxide promoted ZrO_2 catalyst system showed that the Mo/ZrO_2 prepared by impregnating $\text{Zr}(\text{OH})_2$ with the solution of ammonium heptamolybdate and then drying and calcining at 973–1073 K is a solid superacid [1,2,10,11], while Mo/ZrO_2 prepared by impregnating the crystallized ZrO_2 and then drying and calcining is only a catalyst for partial oxidation [45]. It was also reported [1,2,10,11] that ZrO_2 is tetragonal in the former and monoclinic in the latter. In the case of molybdenum-oxide/zirconia solid superacids, zirconia exists as metastable tetragonal modification, which has a large specific surface area and easily combines with MoO_3 to form the Mo–O–Zr surface species. As the Mo-oxide loading exceeds to a certain level, the Mo–O–Zr surface species develops into the bulk $\text{Zr}(\text{MoO}_4)_2$. Similar analogy can be extrapolated to the present molybdate/titania–zirconia catalyst

system, where the doped Mo-oxide interacts strongly with the ZrO_2 portion of the $\text{TiO}_2\text{-ZrO}_2$ mixed oxide and readily forms $\text{Zr}(\text{MoO}_4)_2$ compound. The XPS binding energies and extensive broadening of the Mo 3d lines indicate the presence of intermediate Mo–O–Zr or MoO_x species. In the case of tungsten-oxide promoted ZrO_2 catalysts, several interesting papers can be found in the literature [37,43]. In particular, the surface structure of the dispersed tungsten oxide was reported to change with loading and calcination temperature [37]. The observed strong acidic properties of the W/ZrO_2 catalyst were mainly attributed to the formation of a poorly defined WO_x overlayers on ZrO_2 consisting of Keggin-type structures in a similar way as in heteropolyanions [37]. Similar analogy can also be extended to the present catalyst system, where the

dispersed W-oxide interacts with the binary oxide support and forms a structure similar to the one observed in the case of Mo-oxide/TiO₂-ZrO₂ catalysts. In view of the structural similarities, all these materials exhibit very strong solid acidity.

4. Conclusions

The following conclusions can be drawn from this investigation. (1) the TiO₂-ZrO₂ binary oxide, X-ray amorphous at 773 K, gets converted into ZrTiO₄ compound when calcined at 1073 K and this compound is thermally quite stable in the absence of any promoter atoms. (2) The incorporated sulfate, molybdate, and tungstate promoters exhibit a strong influence on the physicochemical properties of the TiO₂-ZrO₂ mixed oxide. The XRD studies further indicate the formation of Ti₂(SO₄)₃ and Zr(SO₄)₂ in the case of SO₄²⁻ incorporated samples and Zr(MoO₄)₂ and Zr(WO₄)₆, respectively, in the case of Mo- and W-oxide doped samples. (3) The XPS intensities of the O 1s, Ti 2p, and Zr 3d lines and their binding energies indicate that the sulfate ion strongly interacts with the support surface followed by molybdenum oxide. (4) The XPS binding energies of the Mo 3d and W 4f lines and their peak broadening indicate that the binary oxide support contains, in addition to the well-defined Zr compounds of Mo and W, an undefined MoO_x and WO_x phases on the surface of the support. Finally, further studies are highly essential in order to understand the surface structure of these interesting catalytic materials.

Acknowledgements

B.M.R. acknowledges a senior STA visiting fellowship from the Japan Science and Technology Corporation (JST). We thank Drs. A. Ueda and H. Ando for useful discussions.

References

- [1] K. Arata, Adv. Catal. 37 (1990) 165 and references therein.
- [2] K. Arata, M. Hino, Mater. Chem. Phys. 26 (1990) 213 and references therein.
- [3] M. Hino, K. Arata, Chem. Lett. (1980) 963.
- [4] K. Arata, M. Hino, Bull. Chem. Soc. Jpn. 53 (1980) 446.
- [5] K. Arata, K. Yabe, I. Toyoshima, J. Catal. 44 (1976) 385.
- [6] M. Hino, K. Arata, Chem. Lett. (1981) 1671.
- [7] K. Arata, I. Toyoshima, Chem. Lett. (1974) 929.
- [8] G.A. Olah, G.K.S. Prakash, J. Sommer, Science 13 (1979) 206.
- [9] G.A. Olah, G.K.S. Prakash, J. Sommer, Superacids, Wiley, New York, 1985.
- [10] M. Hino, K. Arata, J. Chem. Soc. Chem. Commun. (1988) 1259.
- [11] K. Arata, M. Hino, Chem. Lett. (1989) 971.
- [12] B. Manohar, V.R. Reddy, B.M. Reddy, Synth. Commun. 28 (1998) 3183.
- [13] B.M. Reddy, V.R. Reddy, Synth. Commun. 29 (1999) 2789.
- [14] B.M. Reddy, V.R. Reddy, D. Giridhar, Synth. Commun. 31 (2001) 1819.
- [15] K. Tanabe, H. Hattori, T. Yamaguchi, Stud. Surf. Sci. Catal. 51 (1989) 199.
- [16] X. Song, A. Sayari, Catal. Rev. Sci. Eng. 38 (1996) 329.
- [17] J. Fung, I. Wang, J. Catal. 130 (1991) 577.
- [18] B.M. Reddy, B. Manohar, S. Mehdi, J. Solid State Chem. 97 (1992) 233.
- [19] B.M. Reddy, B. Chowdhury, P.G. Smirniotis, Appl. Catal. A: Gen. 211 (2001) 19.
- [20] W.M. Mullins, B. Averbach, Surf. Sci. 206 (1988) 29.
- [21] US Patent 5,576,467 (1996).
- [22] I. Wang, W.H. Huang, C. Wu, Appl. Catal. 18 (1985) 273.
- [23] B.M. Reddy, B. Chowdhury, E.P. Reddy, A. Fernández, J. Mol. Catal. A: Chem. 162 (2000) 423.
- [24] D. Briggs, M.P. Seah (Eds.), Practical Surface Analysis, Auger and X-Ray Photoelectron Spectroscopy, Vol. 1, 2nd Edition, Wiley, New York, 1990.
- [25] C.D. Wagner, W.M. Riggs, L.E. Davis, J.F. Moulder, in: G.E. Muilenberg (Ed.), Handbook of X-Ray Photoelectron Spectroscopy, Perkin-Elmer Corporation, Minnesota, 1978.
- [26] B.M. Reddy, B. Chowdhury, J. Catal. 179 (1998) 413.
- [27] T. Noguchi, M. Mizuno, Sol. Energy 11 (1967) 56.
- [28] J.C. Wu, S.C. Chung, A.Y. Ching-Lan, I. Wang, J. Catal. 87 (1984) 98.
- [29] I.R. Beattie, T.R. Gilson, J. Chem. Soc. A (1969) 2322.
- [30] D.A. Powers, H.B. Gray, Inorg. Chem. 12 (1973) 2721.
- [31] M. Kilo, Ch. Schild, A. Wokaun, A. Baiker, J. Chem. Soc., Faraday Trans. 88 (1992) 1453.
- [32] J. Miciukiewicz, T. Mang, H. Knözinger, Appl. Catal. A: Gen. 122 (1995) 151.
- [33] R.B. Quincy, M. Houalla, D.M. Hercules, J. Catal. 106 (1987) 85.
- [34] I.E. Wachs, F.D. Hardcastle, Catalysis, Vol. 10, The Royal Society of Chemistry, Cambridge, 1993, p. 102.
- [35] B. Zhao, X. Wang, H. Ma, Y. Tang, J. Mol. Catal. A: Chem. 108 (1996) 167.
- [36] J.A. Horsley, I.E. Wachs, J.M. Brown, G.H. Via, F.D. Hardcastle, J. Phys. Chem. 91 (1987) 4014.
- [37] M. Scheithauer, R.K. Grasselli, H. Knözinger, Langmuir 14 (1998) 3019.
- [38] N.K. Nag, J. Phys. Chem. 91 (1987) 2324.
- [39] G.A. Sawatzky, D. Prost, Phys. Rev. B20 (1979) 1546.

- [40] C.D. Wagner, L.H. Gale, R.H. Raymond, *Anal. Chem.* 51 (1979) 466.
- [41] B.J. Lindberg, K. Hamrin, G. Johansson, U. Gelius, A. Fahlmann, C. Nordling, K. Siegbahn, *Phys. Sci.* 1 (1970) 277.
- [42] P. Biloen, G.T. Pott, *J. Catal.* 30 (1973) 169.
- [43] C.D. Baertsch, S.L. Soled, E. Iglesia, *J. Phys. Chem. B* 105 (2001) 1320.
- [44] D.A. Ward, E.I. Ko, *J. Catal.* 150 (1994) 18.
- [45] H. Miyata, S. Tokuda, T. Ono, *J. Chem. Soc., Faraday Trans.* 1 (86) (1990) 2291.